Natural Resources Canada | Ressources naturelles Canada

GEOLOGICAL SURVEY OF CANADA

CANADIAN GEOSCIENCE MAP 261E

CANADA-NUNAVUT GEOSCIENCE OFFICE

OPEN FILE MAP 2016-18E

GEOLOGY

IRVINE INLET (NORTH)

Baffin Island, Nunavut

Map Information Document

Preliminary

Geological Survey of Canada Canadian Geoscience Maps

2016

Canada

PUBLICATION

CANADA-NUNAVUT GEOSCIENCE OFFICE
BUREAU GÉOSCIENTIFIQUE CANADA-NUNAVUT
ᑲᓇᑕᐅᔪᓂ-ᓄᓇᕗᑦ ᑲᑎᒪᔨᖏᑦᑐᖅ
KANATAMI-NUNAVUMI GEOSCIENCE TITIGAKVIIT

Map Number

Natural Resources Canada, Geological Survey of Canada
Canadian Geoscience Map 261E (Preliminary),
Canada-Nunavut Geoscience Office
Open File Map 2016-18E

Title

Geology, Irvine Inlet (North), Baffin Island, Nunavut

Scale

1:100 000

Catalogue Information

Catalogue No. M183-1/261-2016E-PDF
ISBN 978-0-660-04144-5
doi:10.4095/297794

Copyright

Recommended Citation

St-Onge, M.R., Weller, O.M., Dyck, B.J., Rayner, N.M., Chadwick T., and Liikane, D., 2016. Geology, Irvine Inlet (north) , Baffin Island, Nunavut; Geological Survey of Canada, Canadian Geoscience Map 261E (preliminary); Canada-Nunavut Geoscience Office, Open File Map 2016-18E, scale 1:100 000. doi:10.4095/297794

ABSTRACT

This map summarizes the field observations for the Irvine Inlet (north) map area following eight weeks of regional and targeted bedrock mapping on western Hall Peninsula. The 2015 field campaign completes a two-decade mission to update map coverage for the whole of Baffin Island south of latitude 70°N. The bedrock is dominated by a Paleoproterozoic metaplutonic suite, ranging in composition from gabbro to syenogranite, with crosscutting relations indicating a progression from mafic to silicic magmatism. Prevailing upper amphibolite to lower granulite facies metamorphic conditions overlap the stability limits of magnetite and orthopyroxene, which is consistent with equilibrium phase diagrams and regional aeromagnetic data. Metasedimentary rocks, including quartzite, pelite, marble, and metagreywacke, are present as screens and enclaves between and within plutonic bodies. An examination of the 'ghost' stratigraphy suggests that the metasedimentary rocks can be correlated with the middle Paleoproterozoic Lake Harbour Group in the south and Piling Group in the north. Two basaltic dyke swarms and shallowly dipping Ordovician limestone respectively crosscut and overly the Paleoproterozoic units.

RÉSUMÉ

La présente carte synthétise les observations de terrain réalisées dans la région cartographique d'Irvine Inlet (nord) suite à huit semaines de cartographie régionale et ciblée du substratum rocheux. La campagne de terrain de 2015 met fin à deux décennies de travaux visant à mettre à jour la couverture cartographique de l'ensemble de l'île de Baffin au sud de la latitude 70°N. Le substratum rocheux est dominé par une suite métaplutonique du Paléoprotérozoïque, dont la composition varie du gabbro au syénogranite, qui affiche des relations de recoupement révélant une progression d'un magmatisme mafique à un magmatisme siliceux. Les conditions dominantes d'un métamorphisme du faciès des amphibolites supérieur au faciès des granulites inférieur chevauchent les limites de stabilité de la magnétite et de l'orthopyroxène, ce qui est compatible avec les diagrammes de phases à l'équilibre et les données aéromagnétiques régionales. Des roches métasédimentaires, dont de la quartzite, de la pélite, du marbre et du metagrauwacke, sont présents sous forme d'écrans entre les massifs plutoniques et d'enclaves au sein de ceux-ci. Une examination de la stratigraphie «fantôme» laisse croire que les roches métasédimentaires peuvent être corrélées avec les unités du Paléoprotérozoïque moyen du Groupe de Lake Harbour, au sud, et du Groupe de Piling, au nord. Deux essaims de dykes basaltiques et des strates de calcaire ordovicien de faible pendage recoupent et recouvrent respectivement les unités de carte d'âge Paléoprotérozoïque.

ABOUT THE MAP

General Information

Authors: M.R. St-Onge, O.M. Weller, B.J. Dyck, N.M. Rayner, T. Chadwick, and D. Liikane

Geology by M.R. St-Onge, O.M Weller, B.J. Dyck, N.M. Rayner, T. Chadwick, and D. Liikane, Geological Survey of Canada; S. Noble-Nowdluk, T. Milton, and T. Rowe, Government of Nunavut, 2015

Geological interpretation by M.R. St-Onge and notes by M.R. St-Onge and O.M. Weller, 2015

Geology conforms to Bedrock Data Model, beta v. 2.6

Geomatics by A. Morin, A. Ford, C. Gilbert, L. Robertson, G. Buller, and R. Buenviaje

Cartography by N. Côté

This map is part of the Geo-mapping for Energy and Minerals (GEM) Program on Baffin Island led by the Geological Survey of Canada (GSC) in collaboration with the Canada-Nunavut Geoscience Office (CNGO), Nunavut Arctic College, Carleton University, the University of Oxford, and the Government of Nunavut.

Logistical support provided by the Polar Continental Shelf Program as part of its mandate to promote scientific research in the Canadian North. PCSP 05615

Map projection Universal Transverse Mercator, zone 19.
North American Datum 1983

Base map at the scale of 1:250 000 from Natural Resources Canada, with modifications.
Elevations in metres above mean sea level

Mean magnetic declination 2016, 30°33’W, decreasing 27.4’ annually.
Readings vary from 30°10’W in the SW corner to 30°55’W in the NE corner of the map.

This map is not to be used for navigational purposes.

Title photograph: Layered hornblende-orthopyroxene-magnetite metagabbro sill. Hammer is 35 cm long. Irvine Inlet, Baffin Island, Nunavut.
Photograph by M.R. St-Onge. 2015-130

The Geological Survey of Canada welcomes corrections or additional information from users.

Data may include additional observations not portrayed on this map.
See documentation accompanying the data.
Additional descriptive notes, references, and figures are included in the map information document.

This publication is available for free download through
GEOSCAN (http://geoscan.nrcan.gc.ca/)
and the Canada-Nunavut Geoscience Office (http://cngo.ca/).

Preliminary publications in this series have not been scientifically edited.

Map Viewing Files

The published map is distributed as a Portable Document File (PDF), and may contain a subset of the overall geological data for legibility reasons at the publication scale.

Cartographic Representations Used on Map

This map utilizes ESRI Cartographic Representations in order to customize the display of standard GSC symbols for visual clarity on the PDF of the map only. The digital data still contains the original symbol from the standard GSC symbol set. The following legend features have Cartographic Representations applied:

Normal fault; solid circle indicates downthrown side
Oblique-slip fault, normal, inferred

ABOUT THE GEOLOGY

How to read the geological map

The objective of mapping south-central Baffin Island in 2015 was to improve the geological knowledge and document the economic potential of the greater Iqaluit area. Geological maps show the distribution of geological features, including different kinds of rocks and faults. Although the geology of every area is different, all geological maps have several features in common: coloured areas and letter symbols to represent the kind of rock unit at the surface, lines to show the type and location of contacts and faults, strike and dip symbols to show which way layers are tilted, and a map legend that explains the colours and symbols utilized.

The most striking features of geological maps are its colours. Each colour represents a different geological unit. A geological unit is a volume of a certain kind of rock of a given age. Geological units are named and defined by the geologists who make the geological map, based on observations of the rocks in the field and investigations on the age of the rocks. In addition to colour, each geological unit is assigned a set of letters to uniquely symbolize it on the map. Usually the symbol is the combination of an initial capital letter followed by one or more capital or lowercase letters. The first capital letter represents the age of the geological unit. Geologists have divided the history of the Earth into Eons. All letter symbols begin with a capital letter representing an Eon: for example P (Paleoproterozoic – 2500 to 1600 million years ago), N (Neoproterozoic – 1000 to 541 million years ago), or Q (Quaternary – 2.58

million years ago until today). The capital letters that follow indicate the name of the unit, if it has one. Lowercase letters indicate the type of rock. An example of named rock units on Baffin Island are metasedimentary rocks named "Lake Harbour Group". So PLHq on the map would be the symbol for Lake Harbour Group quartzite (deposited in the Paleoproterozoic). Similarly, Nd would be the symbol for an unnamed unit of diabase emplaced in the Neoproterozoic.

The place where two different geological units are found next to each other is called a contact, and this is represented by different kinds of lines on the geological map. When different geological units have been moved next to one another after they were formed, the contact is a fault contact. If one rock was intruded into another (for example granite intruded into sedimentary strata) then the contact is an intrusive contact. Another kind of line shown on most geologic maps is a fold axis. In addition to being moved by faults, geological units can also be bent and warped into folds. A line that follows the crest or trough of the fold is called the fold axis. Where the contact line is precisely located, it is shown as a solid line, but where it is uncertain, it is shown as dashed. The lines on the map may be modified by other symbols on the line (triangles, small tick marks, arrows, and more) which give more information about the line. For example, faults with triangles on them show that the side with the triangles has been moved up and over the side without the triangles. All the different symbols on the lines are explained in the map legend. Tilted layers are shown on a geological map with a strike and dip symbol. The symbol consists of three parts: a long line, a short line, and a number. The long line is called the strike line, and shows the direction in the layer that is still horizontal. Any tilted surface has a direction that is horizontal (think about walking on the side of a hill, there is always a way to go that is neither up nor down, but is level). The short line is called the dip line, and shows which way the layer is tilted. The number is called the dip, and shows how much the layer is tilted, in degrees, from flat. The higher the number, the steeper the tilting of the layer. Strike and dip symbols can be modified to give more information about the tilted layers just like lines can be, and these modifications are explained in the map legend.

All geological maps come with a table called a map legend. In the legend, all the colours and symbols are shown and explained. The map legend starts with a list showing the colour and letter symbol of every geological unit, starting at the top with the youngest or most recently formed unit, along with the name of the unit (if it has one) and a short description of the types of rock in that unit and their age. After the list of geological units, all the different types of lines on the map are explained, and then all the different strike and dip symbols. The map legend will also include explanations of any other kind of geological symbols used on a map (for example locations where fossils were found, locations of deposits of precious metals, and any other geological feature that might be important in the area documented by the geological map). Because the geology in every area is different, the map legend is vital to understanding the geological map.

Fieldwork and geological mapping on south-central Baffin Island established the distribution of metasedimentary rocks (Lake Harbour Group; map units PLHq, PLHc, PLHs, PLHp; Piling Group; unit PPL) that can be correlated or not with rock formations

on Meta Incognita Peninsula. A suite of magmatic sheets (sills) was documented and will be the focus of further study (map units PLHu, PLHm, PLHd). These are of potential economic importance as they contain metallic minerals (sulphides), and their occurrence could indicate the presence of economic metal concentrations. Three rock deformations and two thermal events were recognized. Such events can be correlated with similar ones that took place 1800 million years ago and have been previously documented both elsewhere on Baffin Island and in northern Quebec. These results will be used to compare and improve models showing the ancient geological evolution of Nunavut.

Descriptive Notes

INTRODUCTION

The Geo-mapping for Energy and Minerals (GEM) program targeted south-central Baffin Island for strategic, helicopter-assisted bedrock mapping in 2015 (red polygon, Figure 1). The GEM program provides modern, publicly available, regional-scale geoscience knowledge of Canada's north, which supports evidence-based exploration for new energy and mineral resources and enables northern communities to make informed decisions about their land, economy, and society. The 2015 field campaign was particularly significant as it updates the regional bedrock-mapping coverage for the southern half of Baffin Island (south of latitude 70°N), allowing for a new, modern, geoscience understanding of the area. Fieldwork in the region (parts of NTS areas NTS 26-B, -C, -F, -G, -J and -K) was led by the Geological Survey of Canada (GSC) in collaboration with the Canada-Nunavut Geoscience Office (CNGO), and also involved participants from Nunavut Arctic College, Carleton University, the University of Oxford, and the Government of Nunavut.

Initial reconnaissance geological investigations of Baffin Island south of latitude 66°N were carried out from 1949 to 1965, with the data compiled into a regional bedrock map that covered eighteen 1:250 000 NTS map sheets (Blackadar, 1967). This was followed by a series of helicopter-borne operations in central Baffin Island (e.g. Henderson, 1985). More recently, modern geoscience knowledge has been provided by field campaigns featuring helicopter-assisted foot traverses in: southern Baffin Island (1995–1997; green shading, Figure 1), central Baffin Island (2000–2002; orange shading, Figure 1), southwest Baffin Island (2006; yellow shading, Figure 1), Cumberland Peninsula (2009–2011; brown shading, Figure 1), Hall Peninsula (2012–2013; blue shading, Figure 1), and Meta Incognita Peninsula (2014; purple shading, Figure 1). Prior to the summer of 2015, only one section remained to finalize the updated coverage of the whole of Baffin Island south of latitude 70°N: south-central Baffin Island in the Sylvia Grinnell Lake–Clearwater Fiord area (red polygon, Figure 1).

South-central Baffin Island forms part of the northeastern (Quebec-Baffin) segment of the Trans-Hudson Orogen (THO), which is a collisional belt that extends in a broad arcuate shape from northeastern to south-central North America (Hoffman, 1988). The THO formed during the final phase of growth of the Nuna supercontinent, and *sensu lato* records the closure of the Manikewan Ocean between the lower Superior and upper Churchill plates from 1.92 to 1.80 Ga. In detail, the THO is a composite collision zone that involved a series of short-duration tectonothermal events that comprise specific accretionary phases within a much larger orogenic system during

120 Myr of gradual ocean basin closure from ca. 1920 to 1800 Ma (Corrigan et al., 2009; St-Onge et al., 2009). In the southeastern Baffin region, four orogen-scale stacked tectonic levels have been identified (Figure 2). From lowest to highest structural level, these comprise:

1) Archean basement orthogneiss, interpreted as the northern continuation of the Superior craton, and middle Paleoproterozoic supracrustal cover (Povungnituk Group; St-Onge et al., 1996);
2) Middle Paleoproterozoic dominantly monzogranitic and granodioritic orthogneiss, interpreted as a deformed arc-magmatic terrane (Narsajuaq arc; Scott, 1997; St-Onge et al., 2009), or as Narsajuaq-age intrusions in level 3 (Corrigan et al., 2009);
3) Archean basement orthogneiss and middle Paleoproterozoic supracrustal cover (Lake Harbour Group), collectively termed the 'Meta Incognita microcontinent' by St-Onge et al. (2000a), which either represents crust rifted from the Rae or Superior craton, or is exotic to both; and
4) Archean basement orthogneiss, interpreted as the southern continuation of the Rae craton, and middle Paleoproterozoic supracrustal cover (Piling Group; Wodicka et al., 2014), stratigraphically similar to the Hoare Bay Group on Cumberland Peninsula.

Levels 3 and 4 are pervasively intruded by the Cumberland batholith, which comprises various granitoid phases dated at ca. 1865–1845 Ma (Whalen et al., 2010). The Cumberland batholith has been interpreted as an Andean-type batholith (St-Onge et al., 2009), or as the result of post-collisional lithospheric delamination and mantle upwelling (Whalen et al., 2010). All levels are crosscut by ca. 720 Ma basaltic 'Franklin' dykes, which were emplaced during plume magmatism associated with the break-up of the Rodinia supercontinent (Heaman et al., 1992). Levels 3 and 4 are also unconformably overlain by Ordovician limestone strata (Blackadar, 1967).

The four tectonic elements were progressively accreted from the south across a series of north-dipping crustal sutures during extended deformation associated with the THO. The oldest of these sutures, the level 3–4 'Baffin suture', is proposed to have resulted from accretion of the Meta Incognita microcontinent to the Rae craton between ca. 1880 to 1865 Ma (St-Onge et al., 2006). Evidence of this suture is relatively sparse due to post-accretion magmatism engulfing the suture zone, but includes the presence of distinct and opposite-facing stratigraphy (based on regional facies changes) in the area (St-Onge et al., 2009). To the north of the proposed suture is the stratigraphically south-facing Piling Group, which comprises a continental margin sequence, with basal shallow marine continental margin clastic and carbonate platform strata, overlain by a volcano-sedimentary rift package that includes iron-formations and is capped by foredeep turbidites. To the south of the proposed suture is the north-facing Lake Harbour Group, which also comprises a clastic-carbonate continent to foredeep margin sequence, but with notable differences including the presence of a basal orthoquartzite and the absence of iron-formation and metagreywacke. Further evidence for the suture includes thrust imbrication of basement-cover panels in level 3 that pre-date emplacement of the Cumberland batholith (St-Onge et al., 2007). As the 2015 field area

straddles the proposed Baffin suture, one of the major objectives of the campaign was to further investigate this structure.

The level 2–3 ‘Soper River’ suture records the accretion of the Narsajuaq magmatic arc to the Rae-Meta Incognita continental margin. Formation of the suture is bracketed between ca. 1845 Ma, the age of the youngest intra-oceanic phase in the arc (Dunphy and Ludden, 1998), and ca. 1842 Ma, the age of the oldest Andean-type phase (Scott, 1997). Deformation in the hanging wall of the Soper River suture is both extensive and penetrative, and manifest as a regional syn-metamorphic amphibolite- to granulite-facies metamorphic foliation (St-Onge et al., 2007).

The level 1–2 ‘Bergeron’ suture formed during terminal collision of the Superior craton with the amalgamated mosaic of upper-plate terranes (collectively the Churchill plate, or peri-Churchill collage), and is bracketed between ca. 1820 Ma, the age of the youngest dated plutonic unit in the hanging wall of the suture (Scott and Wodicka, 1998), and ca. 1795 Ma, the age of a dyke that crosscuts the suture (Wodicka and Scott, 1997). This event resulted in localised retrograde amphibolite-facies metamorphism of granulite-facies rocks in the upper plate of the collision in southern Baffin Island along reactivated Soper River structures and associated fluid-infiltration zones (St-Onge et al., 2000b).

TECTONOSTRATIGRAPHIC UNITS

Bedrock mapping of the Sylvia Grinnell Lake–Clearwater Fiord area was completed during eight weeks of strategic, helicopter-assisted fieldwork in the summer of 2015. Archean crystalline basement units in the eastern portion of the map area include tonalite and granodiorite gneiss locally intruded by monzogranite, which is locally K-feldspar porphyritic.

Paleoproterozoic metasedimentary strata including quartzite, semipelite, pelite, marble, and greywacke occur as enclaves, screens, and panels within and between various plutons. Mafic-ultramafic bodies are present as sills within the metasedimentary strata.

The bedrock in the area is dominated by a Paleoproterozoic metaplutonic suite ranging in composition from gabbro to syenogranite. Crosscutting relationships define a relative chronology of emplacement for the various phases, which can be broadly summarised as a transition from mafic through to more silicic compositions. The various metaplutonic phases are described in their relative age order below, with a suite of samples collected for U-Pb dating in order to corroborate field crosscutting relationships, and the likely correlation with the Cumberland batholith.

Lastly, minor crosscutting mafic dykes and overlying Ordovician limestone were also mapped in the Sylvia Grinnell Lake–Clearwater Fiord area.

Archean crystalline basement (units Ât–Âmm)

Archean metaplutonic units characterize the bedrock geology of Hall Peninsula and the eastern portion of the Sylvia Grinnell Lake–Clearwater Fiord map area. Gneissic to foliated, fine- to medium-grained biotite±hornblende tonalite to granodiorite commonly

contains layers of diorite to quartz diorite. Massive to foliated, medium grained biotite±magnetite monzogranite, locally K-feldspar porphyritic, is locally crosscut by coarse-grained to pegmatitic syenogranite veins.

Paleoproterozoic metasedimentary (units PLHq–PPL)

Quartzite, semipelite and pelite, psammite (units PLHq–PLHp)

Well-layered and white or rusty weathering quartzite occurs as panels up to several hundred metres thick within monzogranite (Figure 3a, b), and in places is overlain by interbedded psammite, semipelite, and/or pelite (Figure 3b). Quartzite layers range in composition from orthoquartzite to feldspathic quartzite, are strongly recrystallized, and occasionally contain garnet. Pelite horizons contain the assemblage biotite-garnet-sillimanite-K-feldspar-melt (Figure 3c), and typically occur as subordinate layers within biotite±garnet psammitic or biotite±garnet±sillimanite semipelitic migmatite. The primary assemblages contain up to 20 vol. % coarsened leucosome, interpreted as crystallised melt, with patch to stromatic metatexite textures, and are devoid of muscovite, consistent with peak metamorphic conditions that exceeded muscovite-dehydration (St-Onge et al., 2007; Dyck and St-Onge, 2014). Cordierite is also absent from the metasedimentary assemblages, suggesting paleopressures in excess of 6 kbar. Gossanous horizons are common in the siliciclastic units, which locally host chalcopyrite, graphite, and pyrite. Although only seen in restricted windows, the siliciclastic units across most of the field region are lithologically similar to the metasedimentary strata of the contiguous Lake Harbour Group in its type locality (St-Onge et al., 1996, 1998; Scott et al., 1997).

Marble and calc-silicate (unit PLHc)

Calcareous rocks occur as panels up to 100 m thick within the monzogranite, and can be traced for up to 10 km along strike (Figure 3d). The rocks are medium to coarse grained and locally display compositional layering defined by varying proportions of apatite, calcite, diopside, humite, forsterite, magnetite, phlogopite, scapolite, spodumene, titanite, and tremolite (Figure 3e). The calcareous units are considered to represent a tectonostratigraphically higher part of the Lake Harbour Group than the siliclastic units described above.

Metagreywacke (unit PPL)

Metagreywacke is documented in the northeastern part of the field area, occurring as enclaves within a biotite monzogranite (Figure 3f). As noted above, greywacke is not a feature of the type Lake Harbour Group stratigraphy, but is a dominant component of the Longstaff Bluff formation within the Piling Group mapped to the north (Wodicka et al., 2014), suggesting a transition in granitoid host stratigraphy.

Paleoproterozoic mafic-ultramafic sills (units PLHu–PLHd)

Sheets of medium- to coarse-grained, mafic to ultramafic rocks of the Frobisher suite (Liikane et al., 2015) occur throughout the siliciclastic strata of south-central Baffin Island. Individual bodies are typically 10–20 m thick, although some reach one hundred metres in thickness, and extend up to several kilometres along strike. The mafic and ultramafic rocks display sharp, concordant margins with their host metasedimentary units, suggesting that they are sills. Larger bodies are compositionally layered, typified

by a sequence comprising clinopyroxene-orthopyroxene±hornblende metapyroxenite at the base (Figure 4a), followed by olivine-clinopyroxene-orthopyroxene metaperidotite and metagabbro to metaleucogabbro up section (Figure 4b). One of us, Liikane, a senior undergraduate field assistant is conducting a MSc thesis on the petrology, geochemistry, and geochronology of the layered mafic-ultramafic suite and associated mineralization. One of the central questions posed by this thesis is whether the suite is correlative with similar layered intrusions in northern Quebec that are associated with the Raglan Ni-Cu deposit (Figure 2). A more complete description of the mafic-ultramafic rocks is given in Liikane et al. (2015).

Paleoproterozoic metaplutonic suite (units Pg–Psb**)**

Gabbro (unit Pg)

A number of coarse-grained to pegmatitic, kilometre-scale, layered biotite-clinopyroxene-magnetite±hornblende gabbro plutons are present along the western margin of the Sylvia Grinnell Lake–Clearwater Fiord area. In places, the plutons contain lenses of clinopyroxene-bearing anorthosite.

Quartz diorite (unit Pd)

Quartz diorite occurs as a fine-grained, dark weathering, massive to foliated unit containing the assemblage biotite-clinopyroxene-orthopyroxene±hornblende. It is present as discrete plutons in the western part of the field area, and as enclaves within all other units to the east (Figure 5a). Map-scale structural trends indicate that the unit occurs near the stratigraphic base of the metaplutonic suite.

Biotite granodiorite (unit Pgo)

Minor, generally massive, biotite±hornblende±magnetite granodiorite is documented in the northwestern part of the field area. The unit is typically dark weathering and medium grained.

K-feldspar megacrystic biotite monzogranite (units Pmo, Pms, Pmh)

Pink to orange weathering, medium to coarse grained, massive to foliated biotite±orthopyroxene±magnetite±garnet monzogranite with distinctive K-feldspar megacrysts occurs throughout large parts of south-central Baffin Island. K-feldspar phenocrysts form augen up to 10 cm wide, and locally display rapakivi textures (ovoid alkali feldspar mantled by plagioclase feldspar; Figure 5b). The unit is locally reworked by a kilometre-scale north-dipping shear zone in the northern portion of the field area, with σ-porphyroclasts of K-feldspar defining a top-to-the-south thrust sense of shear.

Biotite monzogranite (unit Pmb)

Well-foliated biotite±orthopyroxene±magnetite±hornblende±garnet monzogranite underlies large parts of south-central Baffin Island. The unit is typically medium grained, tan-to-pink weathering and equigranular. The unit alternates between magnetite-rich and magnetite-free domains, and contains hornblende in the northwestern part of the field area. In places, the foliation is observed to be axial planar to isoclinal folding of the unit (Figure 5c), suggestive of widespread shortening across the region.

Garnet-biotite monzogranite (unit Pmg)

White-weathering, massive to foliated, fine- to medium-grained garnet-biotite±magnetite monzogranite occurs predominantly in the eastern portion of the field area. The unit is present as dykes and sills in the K-feldspar megacrystic monzogranite (Figure 3d), and forms plutons that intrude the biotite monzogranite. Garnet is present as abundant 2–30 mm burgundy coloured phenocrysts, frequently in association with biotite (inset, Figure 5d).

Garnet-sillimanite leucogranite (unit PLHw)

Garnet-sillimanite leucogranite occurs as discrete dykes crosscutting the garnet-biotite monzogranite or as map scale plutons spatially associated with garnet-biotite monzogranite in the eastern part of the field area. The unit is typically fine-grained, with 1–5 mm lilac coloured garnet phenocrysts and mats of sillimanite (Figure 5e). The presence of sillimanite suggests that the leucogranite is derived from muscovite-dehydration melting of metasedimentary units as documented elsewhere on southern Baffin Island (e.g. Dyck and St-Onge, 2014), rather than being a highly fractionated component of the plutonic suite.

Biotite syenogranite (unit Psb)

Coarse-grained to pegmatitic, pink weathering biotite syenogranite forms anastomosing dykes in most units (Figure 5f). In places the syenogranite is foliated, but typically the unit is undeformed and crosscuts foliations (Figure 5a). Rarely, the dykes contain phenocrysts of garnet and tourmaline.

Other units

Basaltic dykes (units MCd, Nd)

Two suites of minor 1–20 m wide sub-vertical fine- to medium-grained basaltic dykes containing 1–2 mm plagioclase phenocrysts are present on south-central Baffin (Figure 4c). The dykes are magnetic and consistently trend either at 110–120° (Tschirhart et al., 2015), or approximately north-northeast. The first set is attributed to the widespread Neoproterozoic (ca. 720 Ma) Franklin dyke suite (Heaman et al., 1992), whereas the second set is tentatively correlated with the poorly constrained Mesoproterozoic–Cenozoic Kekertaluk swarm of Buchan and Ernst (2013).

Limestone (unit OA)

Shallowly dipping (<10°) limestone (Blackadar, 1967) of the middle Ordovician Amadjuak Formation occurs as erosional outliers in the southwestern part of the Sylvia Grinnell Lake–Clearwater Fiord area (Figure 2). In places, the limestone is juxtaposed against the plutonic suite by northwest-striking normal faults, which were active during Paleocene rifting of the Davis Strait (Clarke et al., 1989). The limestone is typically composed of medium grey lime mud, and is fossiliferous, with the assemblage including maclurites, gastropods, cephalopods, brachiopods, coral fragments, and crinoid stems (Figure 4d).

EQUILIBRIUM PHASE DIAGRAMS

Phase equilibria modelling of a representative sample of monzogranite from southern Baffin Island was undertaken to investigate the competing effects of pressure,

temperature, and composition (P, T, and X) on the metamorphic mineral assemblage in felsic granitoid units (Weller et al., 2015). Phase relations were calculated across a range of P-T space, centred upon documented regional metamorphic conditions of 6–8 kbar and 700–800°C (St-Onge et al., 2007), with the intent of rationalizing the range of phases documented within the metagranitoid units, rather than refining P-T estimates. All P-T and T-X phase diagrams were constructed using THERMOCALC v3.40 and the internally consistent dataset tc-ds55 (Holland and Powell, 1998; updated to August, 2004). Modelling was performed in the 11 component MnO-Na_2O-CaO-K_2O-FeO-MgO-Al_2O_3-SiO_2-H_2O-TiO_2-Fe_2O_3 system, utilising the high-temperature solid-solution models considered in Weller et al. (2016). Pressure uncertainties for assemblage field boundaries are approximately ±1 kbar at the 2σ level (Powell and Holland, 2008; Palin et al., 2015). Bulk compositions were calculated by modifying whole-rock X-ray fluorescence data presented by Thériault et al. (2001) for a monzogranite sampled from southern Baffin Island (95-D078B), following the technique of Weller et al. (2013).

A P-T diagram calculated for a representative monzogranite sample (sample 95-D078B from Thériault et al., 2001; Figure 6a) reveals few reactions between high variance assemblages across a wide range of P-T space, as is typical of metagranitoid rocks, with only magnetite (blue line) and orthopyroxene (green line) calculated to have limited stability over the considered sub-solidus conditions. Of note, both orthopyroxene and magnetite stability limits are encountered within the P-T range of relevance to south-central Baffin (white dashed outline), consistent with field observations of the discontinuous presence of both phases across the region.

To investigate the effects of H_2O on the assemblage, a T-MH_2O diagram was constructed at a mid-range pressure (7 kbar), with MH_2O varying from 0 to 1 mol. % (Figure 6b). This diagram reveals that with increasing H_2O content, the temperature of orthopyroxene-in (green line) rapidly increases from about 640°C to 810°C, and conversely the solidus decreases from about 810°C to 640°C. Given the relevant temperature range of 600–800°C, the presence of orthopyroxene and absence of partial melt textures in the metagranitoid rocks suggest that the assumption of a relatively anhydrous bulk composition (0.1 mol. % H_2O; orange line, Figure 6b) is appropriate. This result is also consistent with the presence of rapakivi textures in the field area (Figure 5b), which are thought to require H_2O-undersatured conditions to form (Nekvasil, 1991). However, the diagram also reveals that for all moderately anhydrous bulk compositions (<0.2 mol. % H_2O), over which silicate melt would not be stabilized at <800°C, both orthopyroxene and magnetite (blue line) stability are sensitive to MH_2O. Therefore, in addition to the effects of regional P-T variation discussed above, subtle changes in the water content of a typical granitoid composition at the same P-T condition could also have contributed to the noted discontinuous stability of both phases.

In order to determine the effects of XFe^{3+} on the assemblage, a T-XFe^{3+} diagram was constructed at the same mid-range pressure (7 kbar), with XFe^{3+} varying from 0.0 to 0.5 (Figure 6c). This diagram reveals that both magnetite (blue line) and orthopyroxene (green line) stabilities are a strong function of XFe^{3+}, such that variation in XFe^{3+} could also have added to the irregular map distribution of both phases. The

widespread occurrence of magnetite- and orthopyroxene-bearing metagranitoid rocks suggest that moderate values of XFe^{3+} = 0.05–0.25 are the most plausible (a range that includes the assumed value of 0.1; orange line), as both phases are then stabilised within the suggested temperature range.

Regional aeromagnetic data show complex variation in the magnetic properties of the bedrock in the project area (e.g. Figure 6d; Kiss and Tschirhart, 2015a–r). Field investigations of the data suggest that the major driver of this variability is the differential abundance of magnetite, typically within otherwise relatively homogeneous plutons (Tschirhart et al., 2015). The modelling results are consistent with this inference, as they show that subtle changes in P, T, and X for a reference granitoid would manifest in complex magnetite (and orthopyroxene) distributions, with all other phases remaining relatively constant.

DEFORMATION AND METAMORPHISM

D_1 deformation and M_1 metamorphism

The Paleoproterozoic tectonostratigraphic units described above are generally characterized by the development of a pervasive millimetre- to centimetre-scale compositional foliation (S_1) that is shallow to steeply dipping, and invariably parallel to lithological contacts between supracrustal and plutonic units. In metasedimentary strata, S_1 is defined by layers of aligned M_1 biotite, sillimanite, and garnet, alternating with layers of dominantly plagioclase, K-feldspar and quartz. The garnet can be several millimetres in size and appear poikiloblastic. In the metasedimentary units, S_1 is interpreted as a metamorphic enhancement of primary bedding (S_0). In foliated mafic and felsic plutonic units, S_1 is defined by the alternating distribution of dominantly ferromagnesian-rich layers comprising granoblastic, millimetre-scale M_1 orthopyroxene, biotite, magnetite, clinopyroxene, hornblende, and/or garnet, and layers consisting of dominantly plagioclase and quartz±K-feldspar. The alignment of the orthopyroxene, biotite, clinopyroxene, and hornblende highlights the S_1 foliation in metaplutonic units when present. The S_1 fabric is observed to be axial-planar to ~100 m scale isoclinal folds with shallow north- and south-plunging fold axes (Dyck and St-Onge, 2014).

Prograde granulite-facies M_1 metamorphism of the Lake Harbour Group in the western Meta Incognita Peninsula is constrained at ca. 1.84 Ga by St-Onge et al. (2007). Geochronological and petrological studies will be undertaken to test whether the same metamorphic event can be documented in the present map area.

D_2 deformation

In the Ptarmigan Fiord area, D_2 thick-skinned thrusts involve Archean basement orthogneiss and Paleoproterozoic supracrustal rocks (Chadwick et al., 2015). Both in-sequence and out-of-sequence thrusts occur. The D_2 thrust imbricates are characterized by high-strain to mylonitic contacts between supracrustal rocks and structurally overlying basement. An L_2 mineral-stretching lineation, and an S_2 shear fabric that is parallel to the thrust planes are well developed. The thickness of individual imbricates ranges from ~100 to 800 m and the maximum length of individual imbricates is on the order of ~25 km.

D_1 fabrics (including the pervasive S_1 foliation) and D_2 thrust imbricates are reoriented by a set of regional north- to northwest-trending D_2 folds. The D_2 folds range from metre scale to map scale and display a consistent upright to east-verging asymmetry. No mesoscopic fabric development associated with D_2 folding has been documented.

In northern Quebec, crustal-scale D_2 folding of structural levels 1 and 2 is constrained at ca. 1.76 Ga (Lucas and St-Onge, 1992). Lucas and Byrne (1992) proposed that the orogen-parallel folds resulted from continued horizontal compression during postcollisional intracontinental shortening in the northeastern segment of the Trans-Hudson Orogen.

D_3 deformation

Upright refolding of all older structural elements about east- to northeast-trending D_3 fold axes has generated the fold interference, dome-and-basin map pattern most evident in the southern and eastern portions of the Sylvia Grinnell Lake–Clearwater Fiord area. The interference of D_2 and D_3 folds also generated sufficient structural relief to allow for the study of the crustal architecture of southern Baffin Island, including the three principal structural levels exposed at the present-day erosion surface (Figure 2). The D_3 folding in northern Quebec is constrained between 1.76 and 1.74 Ga (Lucas and St-Onge, 1992).

ECONOMIC CONSIDERATIONS

A number of lithological associations and occurrences with potential economic implications were identified during the 2015 systematic and targeted mapping campaign in the Sylvia Grinnell Lake–Clearwater Sound area. The layered mafic-ultramafic sills emplaced in sulphidic siliciclastic strata may have a lithological context similar to that hosting Ni–Cu–platinum-group element mineralization elsewhere in the Trans-Hudson Orogen (e.g. Raglan deposit in the eastern Cape Smith Belt of northern Quebec; St-Onge and Lucas, 1994; Lesher, 2007). The field characteristics of the sills are described in more detail in Liikane et al. (2015). Serpentinized ultramafic rocks have been identified at a number of localities in the map area, some of which may provide material suitable as carving stone. Other occurrences of interest include sulphide-bearing gossans; and magnetite and semi-precious minerals in marble, including potentially gem-quality apatite and diopside.

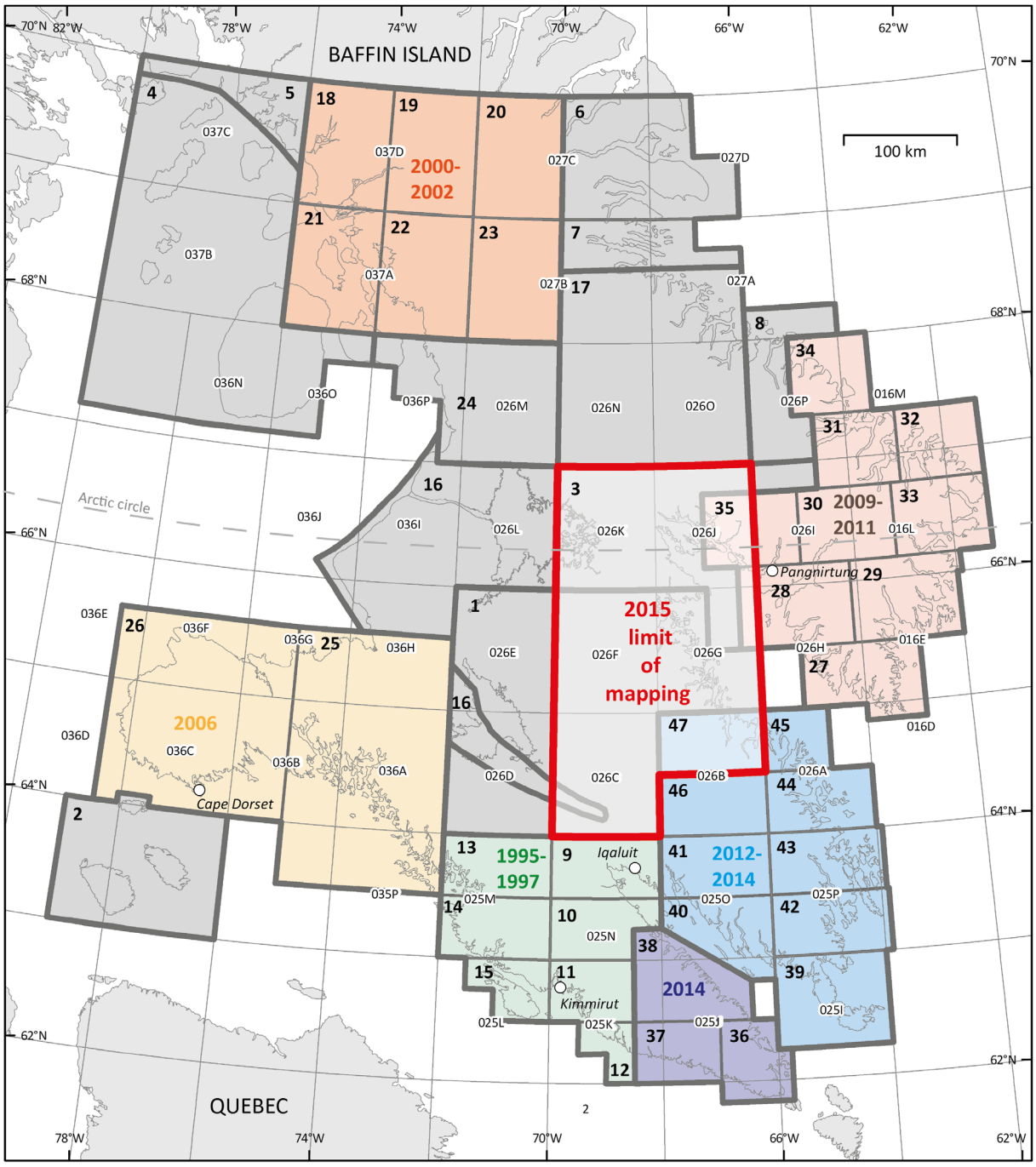

Figure 1. Summary of bedrock mapping campaigns undertaken on Baffin Island, Nunavut. The location of the 2015 south-central Baffin Island field area is shown as a red polygon, and completes the modern mapping coverage south of 70°N. Bold numbers denote map references in chronological order and are listed below. Coloured shading highlights areas and year(s) of recent field campaigns. Alphanumerics refer to National Topographic System map sheets.

1. Blackadar, R.G., 1967. Geology, Cumberland Sound, District of Franklin; Geological Survey of Canada, Preliminary Map 17-1966, scale 1:506 880. doi:10.4095/108490

2. Blackadar, R.G., 1970. Nottingham, Salisbury, and Mill Islands, District of Franklin; Geological Survey of Canada, Map 1205A, scale 1:250 000. doi:10.4095/109212

3. Jackson, G.D., 1971. Operation Penny Highlands, south-central Baffin Island; *in* Report of Activities, Part A: April to October 1970, Geological Survey of Canada, Paper 71-1, Part A, p. 138–140.

4. Trettin, H.P., 1975. Geology, Lower Paleozoic geology, central and eastern parts of Foxe Basin and Baird Peninsula, Baffin Island, District of Franklin; Geological Survey of Canada, Map 1406A, scale 1:500 000. doi:10.4095/109081

5. Morgan, W.C., 1982. Geology, Koch Island, District of Franklin; Geological Survey of Canada, Map 1535A, scale 1:250 000. doi:10.4095/127056

6. Henderson, J.R., 1985a. Geology, McBeth Fiord-Cape Henry Kater, District of Franklin, Northwest Territories; Geological Survey of Canada, Map 1605A, scale 1:250 000. doi:10.4095/120467

7. Henderson, J.R., 1985b. Geology, Ekalugad Fiord-Home Bay, District of Franklin, Northwest Territories; Geological Survey of Canada, Map 1606A, scale 1:250 000. doi:10.4095/120468

8. Jackson, G.D., 1998. Geology, Okoa Bay-Padloping Island area, District of Franklin, Northwest Territories; Geological Survey of Canada, Open File 3532, scale 1:250 000. doi:10.4095/209911

9. St-Onge, M.R., Scott, D.J., and Wodicka, N., 1999a. Geology, Frobisher Bay, Nunavut; Geological Survey of Canada, Map 1979A, scale 1:100 000. doi:10.4095/210833

10. St-Onge, M.R., Scott, D.J., and Wodicka, N., 1999b. Geology, Hidden Bay, Nunavut; Geological Survey of Canada, Map 1980A, scale 1:100 000. doi:10.4095/210835

11. St-Onge, M.R., Scott, D.J., and Wodicka, N., 1999c. Geology, McKellar Bay, Nunavut; Geological Survey of Canada, Map 1981A, scale 1:100 000. doi:10.4095/210836

12. St-Onge, M.R., Scott, D.J., and Wodicka, N., 1999d. Geology, Wright Inlet, Nunavut; Geological Survey of Canada, Map 1982A, scale 1:100 000. doi:10.4095/210840

13. St-Onge, M.R., Scott, D.J., and Wodicka, N., 1999e. Geology, Blandford Bay, Nunavut; Geological Survey of Canada, Map 1983A, scale 1:100 000. doi:10.4095/210837

14. St-Onge, M.R., Scott, D.J., and Wodicka, N., 1999f. Geology, Crooks Inlet, Nunavut; Geological Survey of Canada, Map 1984A, 1:100 000 scale. doi:10.4095/210838

15. St-Onge, M.R., Scott, D.J., and Wodicka, N., 1999g. Geology, White Strait, Nunavut; Geological Survey of Canada, Map 1985A, scale 1:100 000. doi:10.4095/210839

16. Sanford, B.V. and Grant, A.C., 2000. Geological framework of the Ordovician system in the southeast Arctic platform, Nunavut; *in* Geology and Paleontology of the southeast Arctic Platform and southern Baffin Island, Nunavut; Geological Survey of Canada, Bulletin 557, p. 13–38.

17. Jackson, G.D., 2002. Geology, Isurtuq River-Nedlukseak Fiord, Nunavut; Geological Survey of Canada, Open File 4259, scale 1:250 000. doi:10.4095/213304

18. St-Onge, M.R., Scott, D.J., Corrigan, D., and Wodicka, N., 2005a. Geology, Ikpik Bay, Baffin Island, Nunavut; Geological Survey of Canada, Map 2077A, scale 1:100 000. doi:10.4095/221054

19. St-Onge, M.R., Scott, D.J., Corrigan, D., and Wodicka, N., 2005b. Geology, Flyway Lake, Baffin Island, Nunavut; Geological Survey of Canada, Map 2078A, scale 1:100 000. doi:10.4095/221091

20. St-Onge, M.R., Scott, D.J., Corrigan, D., and Wodicka, N., 2005c. Geology, Clyde River, Baffin Island, Nunavut; Geological Survey of Canada, Map 2079A, scale 1:100 000. doi:10.4095/221092

21. St-Onge, M.R., Scott, D.J., Corrigan, D., and Wodicka, N., 2005d. Geology, Piling Bay, Baffin Island, Nunavut; Geological Survey of Canada, Map 2080A, scale 1:100 000. doi:10.4095/221093

22. St-Onge, M.R., Scott, D.J., Corrigan, D., and Wodicka, N., 2005e. Geology, Straits Bay, Baffin Island, Nunavut; Geological Survey of Canada, Map 2081A, scale 1:100 000. doi:10.4095/221094

23. St-Onge, M.R., Scott, D.J., Corrigan, D., and Wodicka, N., 2005f. Geology, Dewar Lakes, Baffin Island, Nunavut; Geological Survey of Canada, Map 2082A, scale 1:100 000. doi:10.4095/221095

24. Jackson, G.D., 2006. Geology, Hantzsch River area, Baffin Island, Nunavut; Geological Survey of Canada, Open File 4202, scale 1:250 000. doi:10.4095/221809

25. St-Onge, M.R., Sanborn-Barrie, M., and Young, M.D., 2007a. Geology, Mingo Lake, Baffin Island, Nunavut; Geological Survey of Canada, Open File 5433, scale 1:250 000. doi:10.4095/224163

26. St-Onge, M.R., Sanborn-Barrie, M., and Young, M.D., 2007b. Geology, Foxe Peninsula, Baffin Island, Nunavut; Geological Survey of Canada, Open File 5434, scale 1:250 000. doi:10.4095/224222

27. Sanborn-Barrie, M., Young, M., Whalen, J., and James, D., 2011a. Geology, Ujuktuk Fiord, Nunavut; Geological Survey of Canada, Canadian Geoscience Map 1 (2nd edition, preliminary), scale 1:100 000. doi:10.4095/289237

28. Sanborn-Barrie, M., Young, M., and Whalen, J., 2011b. Geology, Kingnait Fiord, Nunavut; Geological Survey of Canada, Canadian Geoscience Map 2 (2nd edition, preliminary), scale 1:100 000. doi:10.4095/289238

29. Sanborn-Barrie, M., Young, M., Whalen, J., James, D., and St-Onge, M.R., 2011c. Geology, Touak Fiord, Nunavut; Geological Survey of Canada, Canadian Geoscience Map 3 (2nd edition, preliminary), scale 1:100 000. doi:10.4095/289239

30. Sanborn-Barrie, M. and Young, M., 2013a. Geology, Circle Lake, Nunavut; Geological Survey of Canada, Canadian Geoscience Map 5 (preliminary), scale 1:100 000. doi:10.4095/288929

31. Sanborn-Barrie, M., Young, M., Keim, R., and Hamilton, B., 2013. Geology, Sunneshine Fiord, Nunavut; Geological Survey of Canada, Canadian Geoscience Map 6 (preliminary), scale 1:100 000. doi:10.4095/288931

32. Sanborn-Barrie, M. and Young, M., 2013b. Geology, Padle Fiord, Nunavut; Geological Survey of Canada, Canadian Geoscience Map 37 (preliminary), scale 1:100 000. doi:10.4095/292014

33. Sanborn-Barrie, M. and Young, M., 2013c. Geology, Durban Harbour, Nunavut; Geological Survey of Canada, Canadian Geoscience Map 38 (preliminary), scale 1:100 000. doi:10.4095/292015

34. Sanborn-Barrie, M. and Young, M., 2013d. Geology, Qikiqtarjuaq, Nunavut; Geological Survey of Canada, Canadian Geoscience Map 39 (preliminary), scale 1:100 000. doi:10.4095/292016

35. Jackson, G.D. and Sanborn-Barrie, M., 2014. Geology, Pangnirtung Fiord, Nunavut; Geological Survey of Canada, Canadian Geoscience Map 4 (preliminary), scale 1:100 000. doi:10.4095/288928

36. St-Onge, M.R., Rayner, N.M., Steenkamp, H.M., and Gilbert, C., 2015a. Geology, Terra Nivea, Baffin Island, Nunavut; Geological Survey of Canada, Canadian Geoscience Map 215E (preliminary); Canada-Nunavut Geoscience Office, Open File Map 2015-02E, scale 1:100 000. doi:10.4095/296104

37. St-Onge, M.R., Rayner, N.M., Steenkamp, H.M., and Gilbert, C., 2015b. Geology, Pritzler Harbour, Baffin Island, Nunavut; Geological Survey of Canada, Canadian Geoscience Map 216E (preliminary); Canada-Nunavut Geoscience Office, Open File Map 2015-03E, scale 1:100 000. doi:10.4095/296109

38. St-Onge, M.R., Rayner, N.M., Steenkamp, H.M., and Gilbert, C., 2015c. Geology, Grinnell Glacier, Baffin Island, Nunavut; Geological Survey of Canada, Canadian Geoscience Map 217E (preliminary); Canada-Nunavut Geoscience Office, Open File Map 2015-04E, scale 1:100 000. doi:10.4095/296111

39. Steenkamp, H., Gilbert, C., and St-Onge, M.R., 2016a. Geology, Loks Land, Baffin Island, Nunavut, NTS 25-I (part); Geological Survey of Canada, Canadian Geoscience Map 264 (preliminary); Canada-Nunavut Geoscience Office, Open File Map 2016-01, scale 1:100 000. doi:10.4095/297344

40. Steenkamp, H., Gilbert, C., and St-Onge, M.R., 2016b. Geology, Ward Inlet (south), Baffin Island, Nunavut, NTS 25-O (south) and NTS 25-J (part); Geological Survey of Canada, Canadian Geoscience Map 266 (preliminary); Canada-Nunavut Geoscience Office, Open File Map 2016-02, scale 1:100 000. doi:10.4095/297349

41. Steenkamp, H., Gilbert, C. and St-Onge, M.R., 2016c. Geology, Ward Inlet (north), Baffin Island, Nunavut, NTS 25-O (north); Geological Survey of Canada, Canadian Geoscience Map 265 (preliminary); Canada-Nunavut Geoscience Office, Open File Map 2016-03, scale 1:100 000. doi:10.4095/297348

42. Steenkamp, H., Gilbert, C., and St-Onge, M.R., 2016d. Geology, Beekman Peninsula (south), Baffin Island, Nunavut, NTS 25-P (south) and NTS 15-M (part); Geological Survey of Canada, Canadian Geoscience Map 267 (preliminary); Canada-Nunavut Geoscience Office, Open File Map 2016-04, scale 1:100 000. doi:10.4095/297351

43. Steenkamp, H., Gilbert, C., and St-Onge, M.R., 2016e. Geology, Beekman Peninsula (north), Baffin Island, Nunavut, NTS 25-P (north) and NTS 15-M (part); Geological Survey of Canada, Canadian Geoscience Map 268 (preliminary); Canada-Nunavut Geoscience Office, Open File Map 2016-05, scale 1:100 000. doi:10.4095/297352

44. Steenkamp, H., Gilbert, C., and St-Onge, M.R., 2016f. Geology, Leybourne Islands (south), Baffin Island, Nunavut, NTS 26-A (south); Geological Survey of Canada, Canadian Geoscience Map 269 (preliminary); Canada-Nunavut Geoscience Office, Open File Map 2016-06, scale 1:100 000. doi:10.4095/297353

45. Steenkamp, H., Gilbert, C., and St-Onge, M.R., 2016g. Geology, Leybourne Islands (north), Baffin Island, Nunavut, NTS 26-A (north); Geological Survey of Canada, Canadian Geoscience Map 271 (preliminary); Canada-Nunavut Geoscience Office, Open File Map 2016-07, scale 1:100 000. doi:10.4095/297355

46. Steenkamp, H., Gilbert, C., and St-Onge, M.R., 2016h. Geology, Chidliak Bay (south), Baffin Island, Nunavut, NTS 26-B (south); Geological Survey of Canada, Canadian Geoscience Map 272 (preliminary); Canada-Nunavut Geoscience Office, Open File Map 2016-08, scale 1:100 000. doi:10.4095/297357

47. Steenkamp, H., Gilbert, C., and St-Onge, M.R., 2016i. Geology, Chidliak Bay (north), Baffin Island, Nunavut, NTS 26-B (north); Geological Survey of Canada, Canadian Geoscience Map 270 (preliminary); Canada-Nunavut Geoscience Office, Open File Map 2016-09, scale 1:100 000. doi:10.4095/297354

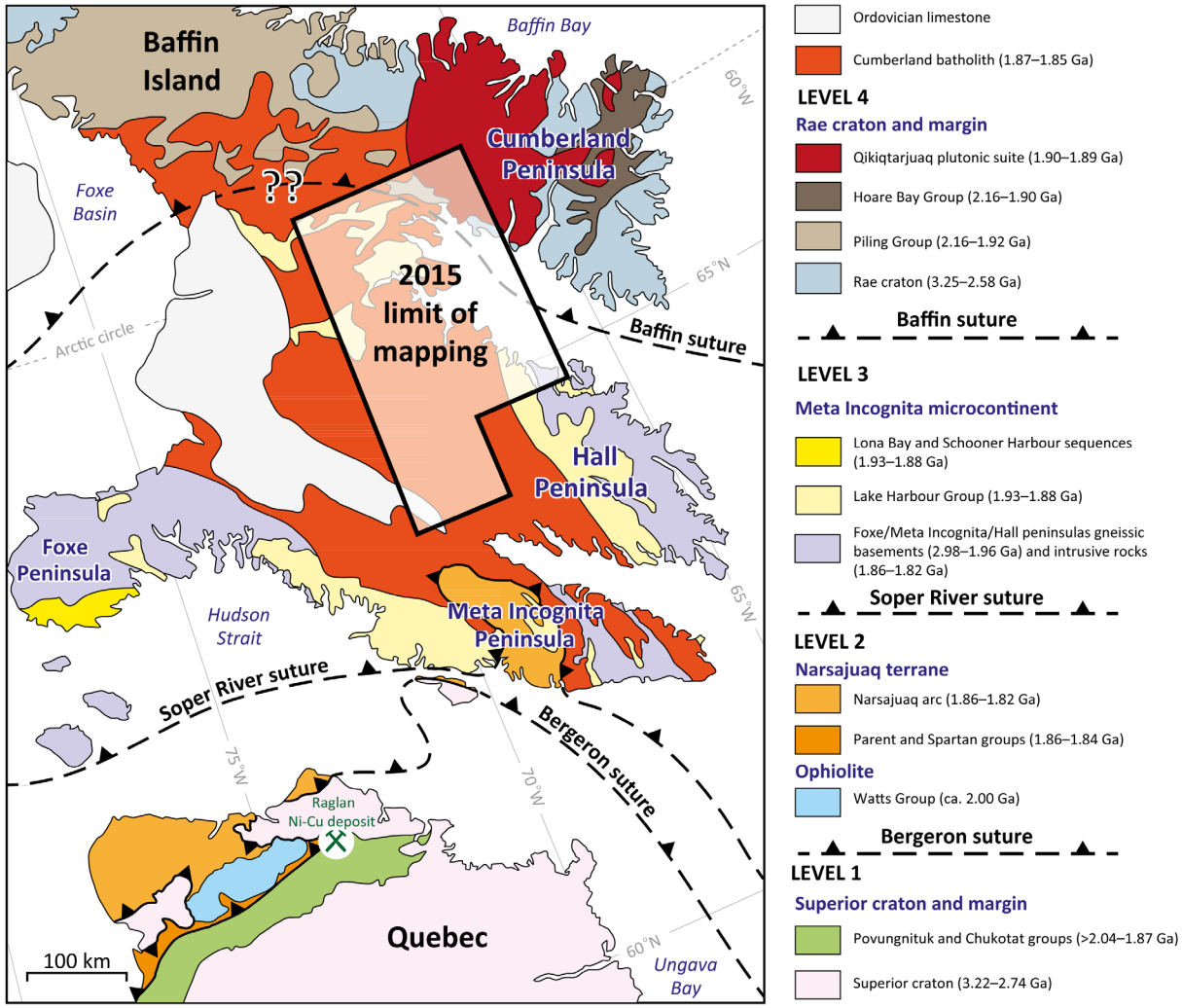

Figure 2. Simplified geological terrane map of the Quebec–Baffin segment of the Trans-Hudson Orogen (*modified after* St-Onge et al., 2007), showing the four structural levels and three sutures. The map provides a regional tectonic context for the south-central Baffin field area, which is outlined in black.

Figure 3. Representative photos of metasedimentary units in the Sylvia Grinnell Lake–Clearwater Fiord area. Alphanumeric in upper-right hand corner of each photograph refers to the 15SAB- field station. a) 10 m panel of rusty-weathered quartzite in biotite monzogranite. b) Well-layered quartzite interbedded with pelite/semipelite. c) Close-up of the pelite/semipelite, showing 1–2 cm garnet porphyroblasts wrapped by a foliation containing biotite and sillimanite. d) Enclave of marble within biotite-orthopyroxene monzogranite. e) Left: magnetite horizon in marble, right: banding in marble caused by varying amounts of humite, diopside and phlogopite. f) Enclave of metagreywacke in biotite monzogranite.

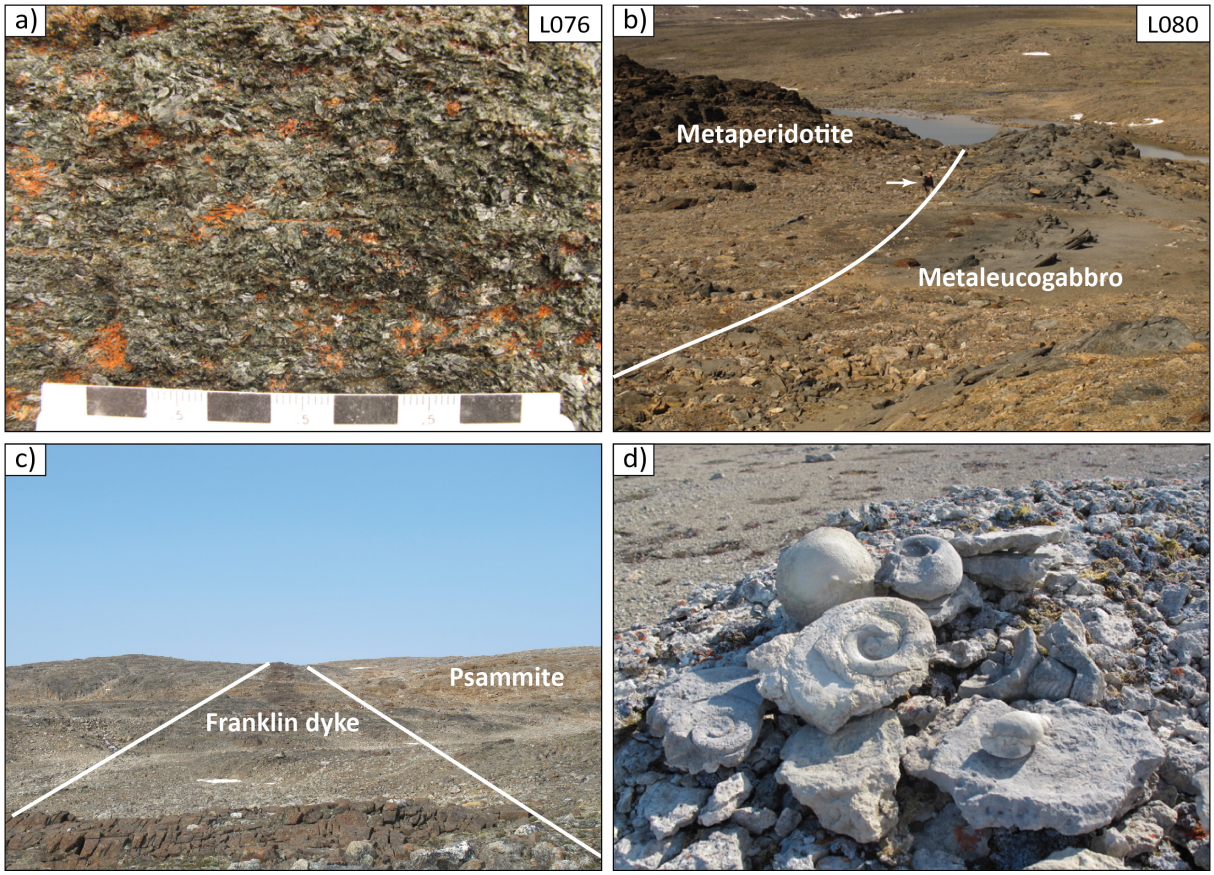

Figure 4. Representative photos of other units in the Sylvia Grinnell Lake–Clearwater Fiord area. Where relevant, the alphanumeric in the upper-right hand corner of each photograph refers to the 15SAB- field station. a) Close-up of a metaclinopyroxenite at the base of a layered mafic sill. Darker regions correspond to minor retrogression to hornblende. b) Central-upper portion of a layered mafic sill, showing brown-weathering metaperidotite capped by grey-weathering metaleucogabbro. Geologist for scale (arrowed) is 1.8 m tall. c) Lake Harbour Group psammite crosscut by a Franklin dyke, with characteristic chocolate-brown weathering and columnar jointing of the latter. Dyke is approximately 10 m in width. d) Typical knobbly weathered surface of limestone, show-casing fossils collected from the wider outcrop. Field of view in foreground is 50 cm.

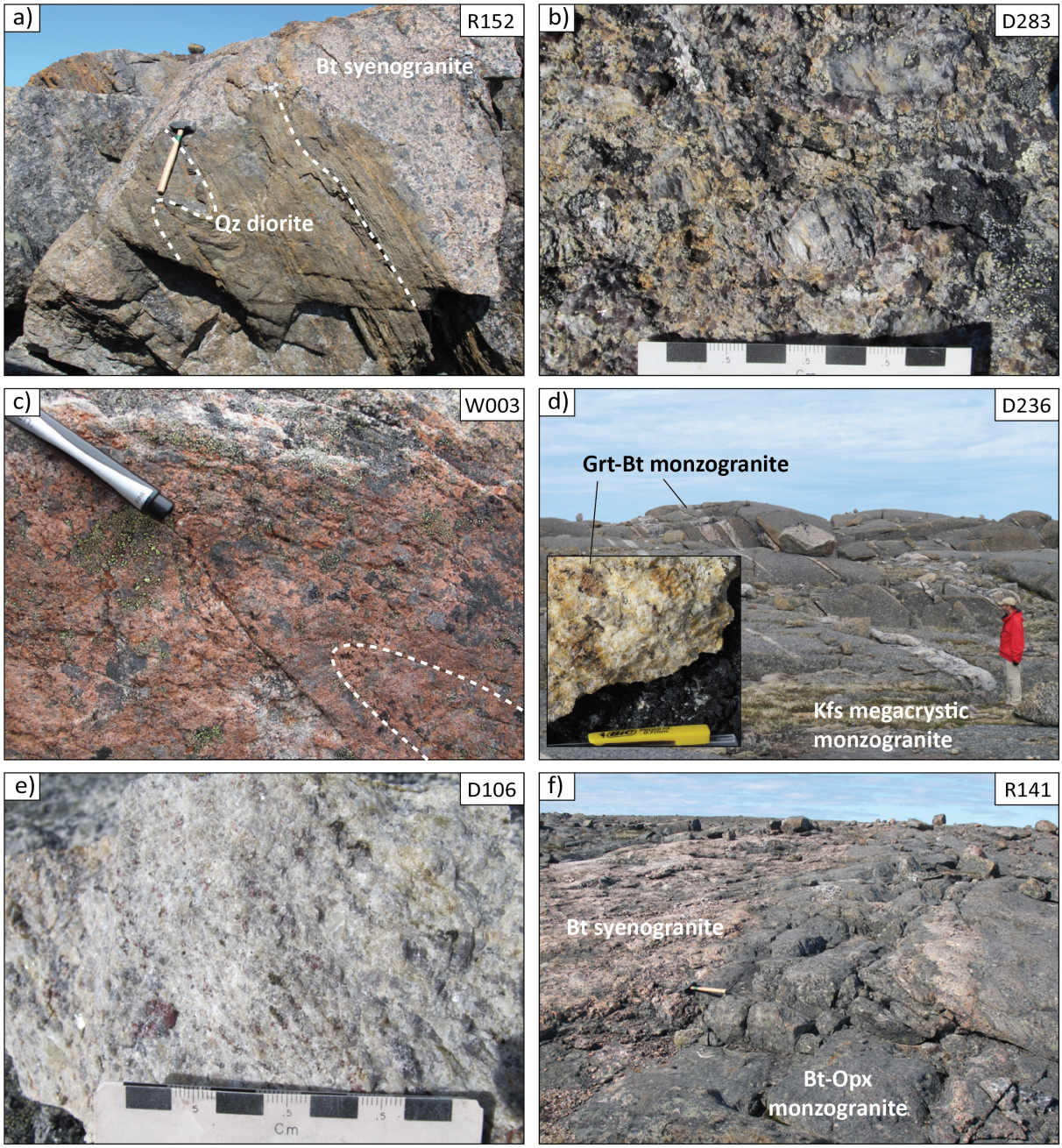

Figure 5. Representative photos of metagranitoid units from the Sylvia Grinnell Lake–Clearwater Fiord area. Alphanumeric in upper-right hand corner of each photograph refers to the 15SAB- field station. a) Enclave of folded and foliated quartz diorite in massive, coarse-grained biotite syenogranite. b) Close-up of the K-feldspar megacrystic monzogranite showing 3–6 cm zoned feldspar augen displaying rapakivi texture. c) Isoclinally folded biotite-orthopyroxene monzogranite. d) Massive K-feldspar megacrystic monzogranite crosscut by a series of sub-parallel biotite-garnet monzogranite dykes. Geologist for scale is 1.8 m tall. Inset: close-up of a biotite-garnet monzogranite sample, showing 1–3 cm burgundy coloured garnet phenocrysts and a weak foliation defined by sub-parallel biotite flakes. e) Close-up of a garnet-sillimanite leucogranite, showing abundant pinprick-sized lilac coloured garnet. f) Massive biotite-orthopyroxene monzogranite crosscut by a network of anastomosing biotite syenogranite dykes. Hammer for scale is 35 cm long.

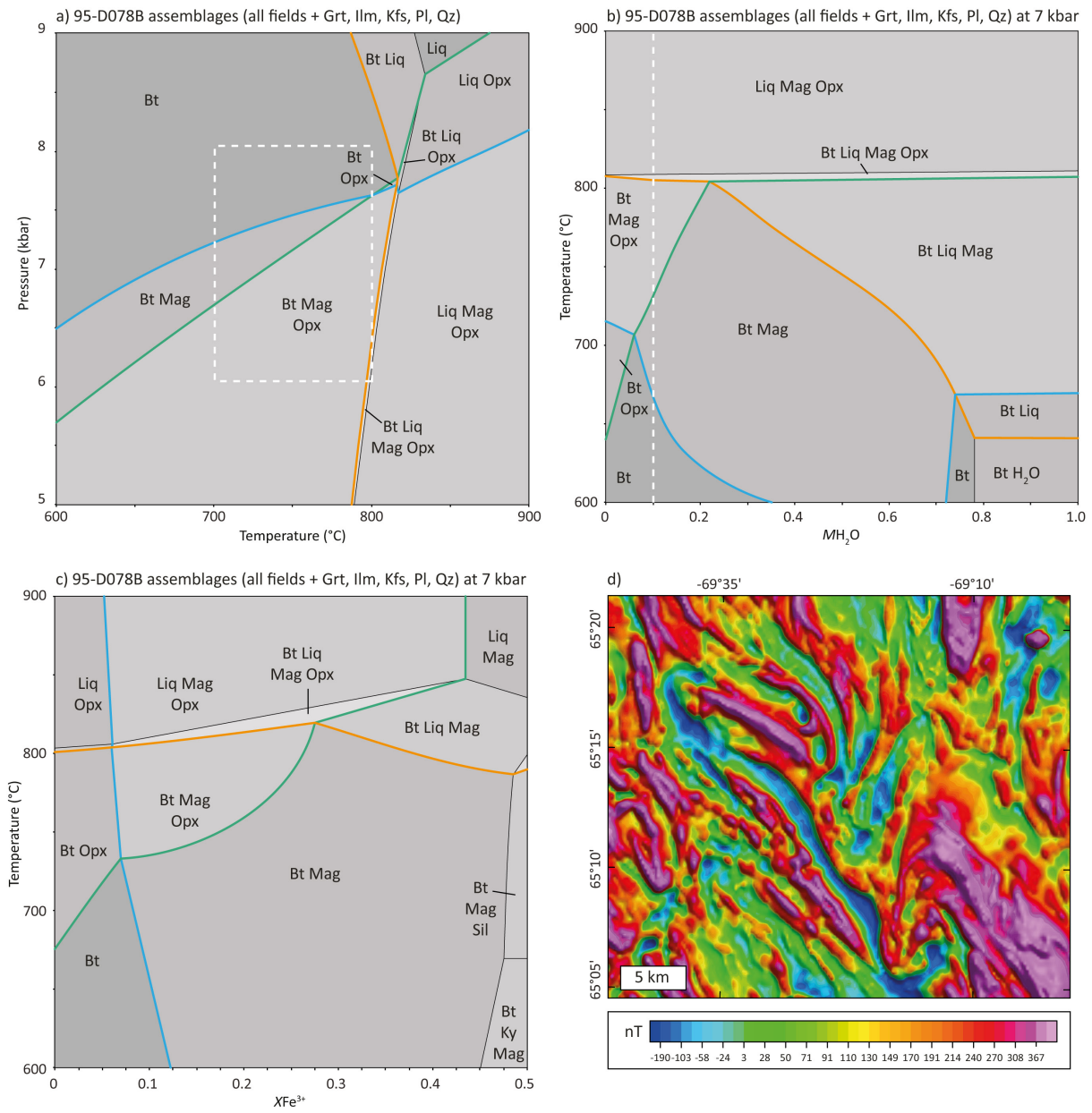

Figure 6. Equilibrium phase diagrams for a representative sample of monzogranite, exploring metagranitoid amphibolite-granulite phase relations: a) P-T diagram; b) T-MH_2O diagram; c) T-XFe^{3+} diagram; d) Residual total field over biotite±magnetite±orthopyroxene monzogranite in field area.

References

Blackadar, R.G., 1967. Geological Reconnaissance, southern Baffin Island, District of Franklin; Geological Survey of Canada, Paper 66-47, 32 p. doi:10.4095/100926

Buchan, K.L. and Ernst, R.E., 2013. Diabase dyke swarms of Nunavut, Northwest Territories and Yukon, Canada; Geological Survey of Canada, Open File 7464. doi:10.4095/293149

Chadwick, T.C., St-Onge, M.R., Weller, O.M., Carr, S.D., and Dyck, B.J., 2015. Ptarmigan Fiord basement–cover thrust imbricates, Baffin Island, Nunavut: summary of fieldwork; *in* Summary of Activities 2015, Canada-Nunavut Geoscience Office, p. 61–72.

Clarke, D.B., Cameron, B.I., Muecke, G.K., and Bates, J.L., 1989. Early Tertiary basalts from the Labrador Sea and Davis Strait region; Canadian Journal of Earth Sciences, v. 26, p. 956–968.

Corrigan, D., Pehrsson, S., Wodicka, N., and de Kemp, E., 2009. The Palaeoproterozoic Trans-Hudson Orogen: a prototype of modern accretionary processes; *in* Ancient Orogens and Modern Analogues, J.B. Murphy, J.D. Keppie, and A.J. Hynes (ed.), The Geological Society, London, Special Publications, v. 327, p. 457–479. doi:10.1144/SP327.19

Dunphy, J.M. and Ludden, J.N., 1998. Petrological and geochemical characteristics of a Paleoproterozoic magmatic arc (Narsajuaq Terrane, Ungava Orogen, Canada) and comparisons to Superior Province granitoids; Precambrian Research, v. 91, p. 109–142.

Dyck, B.J. and St-Onge, M.R., 2014. Dehydration-melting reactions, leucogranite emplacement and the Paleoproterozoic structural evolution of Hall Peninsula, Baffin Island, Nunavut; *in* Summary of Activities 2013, Canada-Nunavut Geoscience Office, p. 73–84.

Heaman, L.M., LeCheminant, A.N., and Rainbird, R.H., 1992. Nature and timing of Franklin igneous events, Canada: implications for a Late Proterozoic mantle plume and the break-up of Laurentia; Earth and Planetary Science Letters, v. 109, p. 117–131.

Henderson, J.R., 1985. Geology, McBeth Fiord-Cape Henry Kater, District of Franklin, Northwest Territories; Geological Survey of Canada, Map 1605A, scale 1:250 000. doi:10.4095/120467

Hoffman, P.F., 1988. United Plates of America, the birth of a craton: Early Proterozoic assembly and growth of Laurentia; Annual Reviews of Earth and Planetary Sciences, v. 16, p. 543–603.

Holland, T.J.B. and Powell, R., 1998. An internally consistent thermodynamic dataset for phases of petrological interest; Journal of Metamorphic Geology, v. 16, p. 309–343.

Kiss, F. and Tschirhart, V., 2015a. Residual total magnetic field, aeromagnetic survey of the Amittok Lake area, Baffin Island, Nunavut, NTS 26-J south; Geological Survey of Canada, Open File 7888, scale 1:100 000. doi:10.4095/296504

Kiss, F. and Tschirhart, V., 2015b. First vertical derivative of the magnetic field, aeromagnetic survey of the Amittok Lake area, Baffin Island, Nunavut, NTS 26-J south; Geological Survey of Canada, Open File 7889, scale 1:100 000. doi:10.4095/296505

Kiss, F. and Tschirhart, V., 2015c. Residual total magnetic field, aeromagnetic survey of the Amittok Lake area, Baffin Island, Nunavut, NTS 26-K south; Geological Survey of Canada, Open File 7890, scale 1:100 000. doi:10.4095/296506

Kiss, F. and Tschirhart, V., 2015d. First vertical derivative of the magnetic field, aeromagnetic survey of the Amittok Lake area, Baffin Island, Nunavut, NTS 26-K south; Geological Survey of Canada, Open File 7891, scale 1:100 000. doi:10.4095/296507

Kiss, F. and Tschirhart, V., 2015e. Residual total magnetic field, aeromagnetic survey of the McKeand River area, part of NTS 26-B/North, Nunavut; Geological Survey of Canada, Open File 7819, scale 1:100 000. doi:10.4095/296382

Kiss, F. and Tschirhart, V., 2015f. First vertical derivative of the magnetic field, aeromagnetic survey of the McKeand River area, part of NTS 26-B/North, Nunavut; Geological Survey of Canada, Open File 7820, scale 1:100 000. doi:10.4095/296383

Kiss, F. and Tschirhart, V., 2015g. Residual total magnetic field, aeromagnetic survey of the McKeand River area, part of NTS 26-C/South, Nunavut; Geological Survey of Canada, Open File 7821, scale 1:100 000. doi:10.4095/296384

Kiss, F. and Tschirhart, V., 2015h. First vertical derivative of the magnetic field, aeromagnetic survey of the McKeand River area, part of NTS 26-C/South, Nunavut; Geological Survey of Canada, Open File 7822, scale 1:100 000. doi:10.4095/296385

Kiss, F. and Tschirhart, V., 2015i. Residual total magnetic field, aeromagnetic survey of the McKeand River area, part of NTS 26-C/North, Nunavut; Geological Survey of Canada, Open File 7823, scale 1:100 000. doi:10.4095/296386

Kiss, F. and Tschirhart, V., 2015j. First vertical derivative of the magnetic field, aeromagnetic survey of the McKeand River area, part of NTS 26-C/North, Nunavut; Geological Survey of Canada, Open File 7824, scale 1:100 000. doi:10.4095/296387

Kiss, F. and Tschirhart, V., 2015k. Residual total magnetic field, aeromagnetic survey of the McKeand River area, part of NTS 26-F/South, Nunavut; Geological Survey of Canada, Open File 7825, scale 1:100 000. doi:10.4095/296388

Kiss, F. and Tschirhart, V., 2015l. First vertical derivative of the magnetic field, aeromagnetic survey of the McKeand River area, part of NTS 26-F/South, Nunavut; Geological Survey of Canada, Open File 7826, scale 1:100 000. doi:10.4095/296389

Kiss, F. and Tschirhart, V., 2015m. Residual total magnetic field, aeromagnetic survey of the McKeand River area, part of NTS 26-F/North, Nunavut; Geological Survey of Canada, Open File 7827, scale 1:100 000. doi:10.4095/296390

Kiss, F. and Tschirhart, V., 2015n. First vertical derivative of the magnetic field, aeromagnetic survey of the McKeand River area, part of NTS 26-F/North, Nunavut; Geological Survey of Canada, Open File 7828, scale 1:100 000. doi:10.4095/296391

Kiss, F. and Tschirhart, V., 2015o. Residual total magnetic field, aeromagnetic survey of the McKeand River area, part of NTS 26-G/South, Nunavut; Geological Survey of Canada, Open File 7829, scale 1:100 000. doi:10.4095/296392

Kiss, F. and Tschirhart, V., 2015p. First vertical derivative of the magnetic field, aeromagnetic survey of the McKeand River area, part of NTS 26-G/South, Nunavut; Geological Survey of Canada, Open File 7830, scale 1:100 000. doi:10.4095/296393

Kiss, F. and Tschirhart, V., 2015q. Residual total magnetic field, aeromagnetic survey of the McKeand River area, part of NTS 26-G/North, Nunavut; Geological Survey of Canada, Open File 7831, scale 1:100 000. doi:10.4095/296394

Kiss, F. and Tschirhart, V., 2015r. First vertical derivative of the magnetic field, aeromagnetic survey of the McKeand River area, part of NTS 26-G/North, Nunavut; Geological Survey of Canada, Open File 7832, scale 1:100 000. doi:10.4095/296395

Lesher, C.M., 2007. Ni-Cu-(PGE) deposits in the Raglan area, Cape Smith Belt, New Quebec; *in* Mineral Deposits of Canada: a Synthesis of Major Deposit Types, District Metallogeny, the Evolution of Geological Provinces and Exploration Methods, W.D. Goodfellow (ed.), Geological Association of Canada, Special Publication, v. 5, p. 351–386.

Liikane, D.A., St-Onge, M.R., Kjarsgaard, B.A., Rayner, N.M., Ernst, R.E., and Kastek, N., 2015. Frobisher suite mafic, ultramafic and layered mafic-ultramfic sills, southern Baffin Island; *in* Summary of Activities 2015, Canada-Nunavut Geoscience Office, p. 21–32.

Lucas, S.B. and Byrne, T., 1992. Footwall involvement during arc-continent collision, Ungava orogen, northern Canada; Journal of the Geological Society of London, v. 149, p. 237–248.

Lucas, S.B. and St-Onge, M.R., 1992. Terrane accretion in the internal zone of the Ungava orogen, northern Quebec. Part 2: Structural and metamorphic history; Canadian Journal of Earth Sciences, v. 29, p. 765–782.

Nekvasil, H., 1991. Ascent of felsic magmas and formation of rapakivi; American Mineralogist, v. 76, p. 1279–1290.

Palin, RM., Weller, O.M., Waters, D.J., and Dyck, B., 2015. Quantifying geological uncertainty in metamorphic phase equilibria modelling; a Monte Carlo assessment and implications for tectonic interpretations; Geoscience Frontiers. doi:10.1016/j.gsf.2015.08.005

Powell, R. and Holland, T.J.B., 2008. On thermobarometry; Journal of Metamorphic Geology, v. 26, p. 155–179.

Scott, D.J., 1997. Geology, U-Pb, and Pb-Pb geochronology of the Lake Harbour area, southern Baffin Island: implications for the Paleoproterozoic tectonic evolution of north-eastern Laurentia; Canadian Journal of Earth Sciences, v. 34, p. 140–155.

Scott, D.J. and Wodicka, N., 1998. A second report on the U-Pb geochronology of southern Baffin Island; Geological Survey of Canada, Current Research 1998-F, p. 47–57.

Scott, D.J., St-Onge, M.R., Wodicka, N., and Hanmer, S., 1997. Geology of the Markham Bay – Crooks Inlet area, southern Baffin Island, Northwest Territories; Geological Survey of Canada, Current Research 1997-C, p. 157–166.

St-Onge, M.R. and Lucas, S.B., 1994. Controls on the regional distribution of iron-nickel-copper-platinum group element sulfide mineralization in the eastern Cape Smith Belt, Quebec; Canadian Journal of Earth Sciences, v. 31, p. 206–218.

St-Onge, M.R., Hanmer, S., and Scott, D.J., 1996. Geology of the Meta Incognita Peninsula, south Baffin Island: tectonostratigraphic units and regional correlations; Geological Survey of Canada, Current Research 1996-C, p. 63–72.

St-Onge, M.R., Scott, D.J. and Lucas, S.B., 2000a. Early partitioning of Quebec: Microcontinent formation in the Paleoproterozoic; Geology, v. 28, p. 323–326.

St-Onge, M.R., Scott, D.J., Wodicka, N., and Lucas, S.B., 1998. Geology of the McKellar Bay – Wight Inlet – Frobisher Bay area, southern Baffin Island, Northwest Territories; Geological Survey of Canada, Current Research 1998-C, p. 43–53.

St-Onge, M.R., Searle, M.P., and Wodicka, N., 2006. Trans-Hudson Orogen of North America and Himalaya-Karakoram-Tibetan Orogen of Asia: Structural and thermal characteristics of the lower and upper plates; Tectonics, v. 25, TC4006, 22p. doi:10.1029/2005TC001907

St-Onge, M.R., Wodicka, N., and Ijewliw, O., 2007. Polymetamorphic evolution of the Trans-Hudson Orogen, Baffin Island, Canada: Integration of petrological, structural and geochronological data; Journal of Petrology, v. 48, p. 271–302. doi:10.1093/petrology/eg1060

St-Onge, M.R., Wodicka, N., and Lucas, S.B., 2000b. Granulite- and amphibolite-facies metamorphism in a convergent plate-margin setting: Synthesis of the Quebec-Baffin segment of Trans-Hudson Orogen. Canadian Mineralogist, v. 38, p. 379–398.

St-Onge, M.R., Van Gool, J.A.M., Garde, A.A., and Scott, D.J., 2009. Correlation of Archaean and Palaeoproterozoic units between northeastern Canada and western Greenland: constraining the pre-collisional upper plate accretionary history of the Trans-Hudson orogen; *in* Earth Accretionary Systems in Space and Time, P.A. Cawood and A. Kroner, The Geological Society, London, Special Publications, v. 318, p. 193–235. doi:10.1144/SP318.7

Thériault, R.J., St-Onge, M.R., and Scott, D.J., 2001. Nd isotopic and geochemical signature of the Paleoproterozoic Trans-Hudson Orogen, southern Baffin Island, Canada: implications for the evolution of eastern Laurentia; Precambrian Research, v. 108, p. 113–138.

Tschirhart, V., St-Onge, M.R., and Weller, O.M., 2015. Preliminary geophysical interpretation of the McKeand River area, Baffin Island, Nunavut: insights from gravity, magnetic and geological data; *in* Summary of Activities 2015, Canada-Nunavut Geoscience Office, p. 49–60.

Weller, O.M., Dyck, B.J., St-Onge, M.R., Rayner, N.M, and Tschirhart, V., 2015. Completing the bedrock mapping of southern Baffin Island, Nunavut: plutonic suites and regional stratigraphy; *in* Summary of Activities 2015, Canada-Nunavut Geoscience Office, p. 33–48.

Weller, O.M., St-Onge, M.R., Rayner, N., Searle, M.P., and Waters, D.J., 2016. Miocene magmatism in the Western Nyainqentanglha mountains of southern Tibet: an exhumed bright spot?; Lithos, doi:10.1016/j.lithos.2015.06.024

Weller, O.M., St-Onge, M.R., Searle, M.P., Rayner, N., Waters, D.J., Chung, S.L., Palin, R.M., Lee, Y.H., and Xu, X.W., 2013. Quantifying Barrovian metamorphism in the Danba Structural Culmination of eastern Tibet; Journal of Metamorphic Geology, v. 31, p. 909–935. doi: 10.1111/jmg.12050

Whalen, J.B., Wodicka, N., Taylor, B.E., and Jackson, G.D., 2010. Cumberland batholith, Trans-Hudson Orogen, Canada: Petrogenesis and implications for Paleoproterozoic crustal and orogenic processes; Lithos, v. 117, p. 99–118. doi:10.1016/j.lithos.2010.02.008

Wodicka, N. and Scott, D.J., 1997. A preliminary report on the U-Pb geochronology of the Meta Incognita Peninsula, southern Baffin Island, Northwest Territories; Geological Survey of Canada, Current Research 1997-C, p. 167–178.

Wodicka, N, St-Onge, M.R., Corrigan, D., Scott, D.J., and Whalen, J.B., 2014. Did a proto-ocean basin form along the southeastern Rae cratonic margin? Evidence from U-Pb geochronology, geochemistry (Sm-Nd and whole rock), and stratigraphy of the Paleoproteorozoic Piling Group, northern Canada; GSA Bulletin, v. 126, p. 1625–1653. doi: 10.1130/B31028.1

Additional information

The Additional Information folder of this product's digital download contains additional geological information not depicted on the PDF of the map, not included in this Map Information Document, or not included in any geodatabase. Additional information refers to an Excel® spreadsheet of the map legend.

Author Contact

Questions, suggestions, and comments regarding the geological information contained in the data sets should be addressed to:

M.R. St-Onge
Geological Survey of Canada
601 Booth Street
Ottawa ON
K1A 0E8
marc.st-onge@canada.ca

Coordinate System

Projection: Universal Transverse Mercator
Units: metres
Zone: 19
Horizontal Datum: NAD83
Vertical Datum: mean sea level

Bounding Coordinates

Western longitude: 68°00'00"W
Eastern longitude: 66°50'00"W
Northern latitude: 66°00'00"N
Southern latitude: 65°30'00"N

Software Version

Data has been originally compiled and formatted for use with ArcGIS™ desktop version 10.1 developed by ESRI®.

Data Model Information

Geological Dataset accompanying this publication complies with the GSC's Project Bedrock Schema (beta version 2.6). A document explaining the data model attributes and domains is available in …\Data\DataModelInfo.

The structure of the XML workspace is not completely consistent with that of shapefiles. For ease of use, shapefiles were exported from the original Bedrock Geodatabase by subtype.

LICENCE AGREEMENT

View the licence agreement at
http://open.canada.ca/en/open-government-licence-canada

ACCORD DE LICENCE

Voir l'accord de licence à
http://ouvert.canada.ca/fr/licence-du-gouvernement-ouvert-canada